Strong solid-state luminescence enhancement in supramolecular assemblies of polyoxometalate and "Aggregation-Induced Emission"-active phospholium

Patricia Bolle, Yohan Cheret, Claire Roiland, Lionel Sanguinet, E. Faulques, H Serier-Brault, Pierre-Antoine Bouit, Muriel Hissler, R Dessapt

Strong solid-state luminescence enhancement in supramolecular assemblies of polyoxometalate and "Aggregation-Induced Emission"-active phospholium

Patricia Bolle,[a] Yohan Chéret,[b] Claire Roiland,[b] Lionel Sanguinet,[c] Eric Faulques,[a] Hélène Serier-Brault,[a] Pierre-Antoine Bouit,*[b] Muriel Hissler,*[b] and Rémi Dessapt*[a]

Abstract: Two new supramolecular fluorescent hybrid materials combining for the first time $[M_6O_{19}]^{2-}$ (M = Mo, W) polyoxometalates (POMs) and the aggregation-induced emission (AIE)-active 1-methyl-1,2,3,4,5-pentaphenyl-phospholium (**1**$^+$) were successfully synthesized. This novel molecular self-assembling strategy allows designing efficient solid-state emitters such as **(1)$_2$[W$_6$O$_{19}$]** by directing favourably the balance between the AIE and aggregation-caused quenching (ACQ) effects using both anion-π^+ and H-bonding interactions in the solid-state. Combined single-crystal X-ray diffraction, Raman, UV-vis and photoluminescence analyses highlighted that the nucleophilic oxygen-enriched POM surfaces strengthened the rigidity of the phospholium via strong C–H···O contacts, thereby exalting its solid-state luminescence. Besides, the bulky POM anions prevented π-π stacking interactions between the luminophores, blocking detrimental self-quenching effects.

Solid-state photoluminescence (PL) of organic compounds has become a topic of intense research in the past decades since many applications from organic electronics (such as Organic Light-Emitting Diodes), to photonics and biological probes are based on this property.[1] Many effort has been spent on defining suitable strategies to develop high-performance solid-state organic emitters. It has been demonstrated that rigid π-conjugated luminophores are highly efficient emitters in diluted solutions but they usually suffer from the aggregation-caused quenching (ACQ) effect in condensed phases due to detrimental π-π stacking interactions between their flat polycyclic rings.[2] Recently, the opposite concept of aggregation-induced emission (AIE)[2] (or aggregation-induced enhanced emission (AIEE)[3]) became highly popular as it describes flexible rotor-like substituted-alkenes (such as tetraphenylethylenes or polyphenyl-heteroles) that are weakly emissive in diluted solutions but show intense luminescence in the aggregated state. This exalted emission mainly results from stiffening of their molecular structure due to restriction of the intramolecular rotations (RIR) of the peripheral rotors that promotes the radiative decay of the excited state. Even if the photophysics of organic solids is more complicated than the duality between opposite AIE and ACQ effects,[4] new strategies have emerged to design high-performance solid-state emitters by directing favorably the AIE/ACQ balance with the use of noncovalent interactions. For example, Tang *et al.* recently reported that anion-π^+ interactions between cationic AIE-oxazoliums and classical PF_6^- counter-ions acting as spacers efficiently reduces the detrimental ACQ effect.[5] In this context, π-conjugated P-heterocycles[6] such as phospholiums appear as promising cationic P-emitters to further extend this approach because they can also exhibit AIE activity when ionically assembled with usual counter-ions (Cl^-, BF_4^-, OTf^-).[7,8] To go further in directing favorably the AIE/ACQ balance in these molecular systems, the use of highly nucleophilic anions able to develop strong H-bonding interactions with phospholiums could be envisioned to strengthen their rigidity, and hence to exalt the AIE effect. Based on this assessment, polyoxometalates (POMs) are promising candidates to efficiently combine both strategies described above. Indeed, these non-conventional redox and optically-active metal-oxide anions[9] exhibit large sizes, high negative charges, and their nucleophilic oxygen surfaces are conducive to develop strong electrostatic and H-bonding interactions with photoactive organic molecules, greatly impacting their photoactivity in the solid-state.[10] For instance, we recently used POMs as efficient structure-directing agents to tune the photoresponses of photochromic spiropyrans[10a] and phosphorescent iridium complexes.[10b] Whereas molecular compounds based on POMs and non-emissive tetraalkylphosphoniums have already been described,[11] the unexplored ionic self-assembly of AIE-active phospholium derivatives with POMs through both anion-π^+ and H-bonding interactions appears as a promising strategy to develop new hybrid organic-inorganic materials with improved solid-state emission properties.

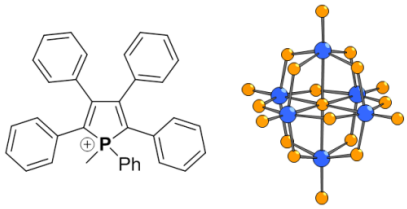

Scheme 1. Representations of the 1-methyl-1,2,3,4,5-pentaphenyl-phospholium (**1**$^+$) (left) and the Lindqvist-type $[M_6O_{19}]^{2-}$ (M = Mo, W) unit (right) considered in this study (blue sphere: Mo or W, orange sphere: oxygen).

As a proof of concept, we describe herein the two first assemblies **(1)$_2$[W$_6$O$_{19}$]** and **(1)$_2$[Mo$_6$O$_{19}$]** combining the AIE emitter 1-methyl-1,2,3,4,5-pentaphenyl-phospholium (**1**$^+$) with Lindqvist-type $[M_6O_{19}]^{2-}$ (M = Mo, W)[12] anions (scheme 1). These archetypal POM units have been chosen due to their high symmetry and their low charge which are suitable features to reach crystallized supramolecular frameworks.

[a] P. Bolle, Dr. H. Serier-Brault, Dr. E. Faulques, Dr. R. Dessapt
Institut des Matériaux Jean Rouxel, UMR 6502
Université de Nantes, CNRS, 2 rue de la Houssinière, BP 32229, 44322 Nantes (France)
E-mail: remi.dessapt@cnrs-imn.fr

[b] Y. Chéret, Dr. C. Roiland, Dr. P.-A. Bouit, Pr. M. Hissler
Univ Rennes, CNRS, ISCR – UMR 6226, ScanMat - UMS 2001, F-35000 Rennes, France
E-mail: pierre-antoine.bouit@univ-rennes1.fr, muriel.hissler@univ-rennes1.fr

[c] Lionel Sanguinet
Université d'Angers, CNRS UMR 6200, Moltech-Anjou, 2 bd Lavoisier, 49045 Angers Cedex (France)
E-mail: lionel.sanguinet@univ-angers.fr

The photophysical properties of **(1)$_2$[W$_6$O$_{19}$]** and **(1)$_2$[Mo$_6$O$_{19}$]** have been thoroughly investigated and compared with those of **(1)[OTf]** in diluted solution and in the solid-state. Structure-property relationships based on combined single-crystal X-ray diffraction, Raman, UV-vis and PL spectroscopy analyses have highlighted that the careful choice of the POM allows designing efficient solid-state emitters. This novel strategy takes advantage of both the size of the POMs and their highly nucleophilic oxygen surfaces to jointly block π-π stacking interactions between the cationic luminophores and to drastically restrict their intramolecular motions, via numerous noncovalent interactions.[5] Besides, considering that POMs can also exhibit intrinsic photophysical properties, these new results thus pave the way toward novel multifunctional hybrid materials.

The elaboration of **(1)[OTf]**, **(1)$_2$[W$_6$O$_{19}$]** and **(1)$_2$[Mo$_6$O$_{19}$]** are fully described in the Supporting Information. **(1)[OTf]** was prepared by methylation of pentaphenylphosphole and characterized by multinuclear solution NMR spectroscopy (Figure S1), solid-state ^{31}P NMR (Figure S2), mass spectrometry, and elemental analysis. Powders of **(1)$_2$[W$_6$O$_{19}$]** and **(1)$_2$[Mo$_6$O$_{19}$]** were synthesized by mixing in acetonitrile $(NBu_4)_2[M_6O_{19}]$ (M = Mo, W) and two folds of **(1)[OTf]**. Their purity was confirmed by elemental analyses, solid-state ^{31}P NMR (Figure S2), and IR (Figure S3) spectroscopies.

Single-crystals were obtained by slow diffusion of pentane into CH_2Cl_2 for **(1)[OTf]**, and by slow diffusion of ethanol into acetonitrile for **(1)$_2$[W$_6$O$_{19}$]** and **(1)$_2$[Mo$_6$O$_{19}$]**. The structures of the three compounds were solved by X-ray diffraction analysis (Table S1). As expected, **1$^+$** adopts a highly twisted conformation in **(1)[OTf]** with torsion angles as large as 38.7-63.0° between the central phosphole core and the peripheral phenyl rings at its 2,3,4,5-positions (Figure S4). Despite the presence of the triflate counter-ions, the **1$^+$** molecules are located in close vicinity. The shorter C···C distance between two nearby **1$^+$** cations is 3.40 Å i.e, the exact sum of two C-atom van der Waals radii, and some of the neighboring phenyl groups are perfectly parallel, characteristic of intermolecular π-π stacking interactions. **(1)$_2$[W$_6$O$_{19}$]** and **(1)$_2$[Mo$_6$O$_{19}$]** are isostructural materials (Table S1), and the structure of **(1)$_2$[W$_6$O$_{19}$]** has been arbitrary chosen to describe the crystal packing of this series. The **1$^+$** molecules are crystallographically equivalent which is well consistent with the single signal (δ = +29.8 ppm) observed by solid-state ^{31}P NMR spectroscopy (Figure S2). As shown in Figure 1a, the $[W_6O_{19}]^{2-}$ and **1$^+$** units are assembled into supramolecular layers in the *bc* plane so that the phosphole stator is quasi parallel to the oxygen facets of the two adjacent POMs (the dihedral angles are 2.7° and 6.8°). Interestingly, in comparison with **(1)[OTf]**, the bulky $[W_6O_{19}]^{2-}$ anions act as large spacers that dilute **1$^+$** in the crystal lattice. Indeed, the **1$^+$** volume concentration is 2.16 .10^{-3} mol/cm^3 in **(1)[OTf]** and drops to 1.94 .10^{-3} mol/cm^3 in **(1)$_2$[W$_6$O$_{19}$]** (1.95 .10^{-3} mol/cm^3 in **(1)$_2$[Mo$_6$O$_{19}$]**) i.e., a decrease of about 11%. Consequently, the shortest C···C distance between two nearby **1$^+$** units increases to 3.60 Å and the phenyl rings are far from being parallel (the smallest dihedral angle is 51°), indicating that the luminophores are no longer involved in direct π-π stacking interactions. **1$^+$** is well surrounded by four adjacent $[W_6O_{19}]^{2-}$ anions (Figure 1b). The phenyl rings and the oxygen POM facets interact via thirteen strong C–H···O contacts with H···O and C···O distances shorter than 2.9 and 3.6 Å, respectively. A fourteenth H-bonding interaction also involves a H-atom of the methyl group. Clearly, all these noncovalent interactions rigidify **1$^+$** and are conducive to greatly impact intramolecular rotations of the phenyl groups.

FT-Raman spectroscopy has been used as a powerful tool to compare the flexibility of **1$^+$** in **(1)[OTf]**, and in the two hybrids, with a particular focus on the range 2800-3200 cm^{-1} (Figure S5) relative to the ν(C-H) stretching vibrations of the phosphole substituents. The FT-Raman spectrum of **(1)[OTf]** (Figure 2a) shows three main bands. The first intense broad one at 3064 cm^{-1} corresponds to the ν(C-H) stretching modes of the phenyl rotors.[13] The two other less intense ones are assigned to the $\nu_s(CH_3)$ symmetric (2915 cm^{-1}) and $\nu_{as}(CH_3)$ asymmetric (2995 cm^{-1}) stretching vibrations of the methyl group.

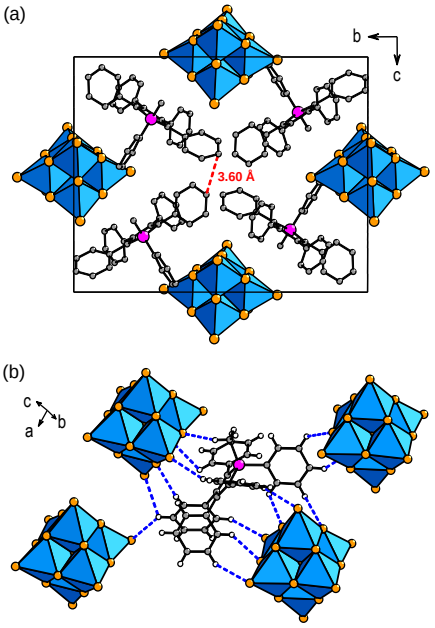

Figure 1. (a) Mixed polyhedral and ball-and-stick representations of the crystal packing in **(1)$_2$[W$_6$O$_{19}$]** (H-atoms are omitted for clarity). The red dotted line corresponds to the shortest intermolecular C···C distance. (b) Representation of the fourteen strong C-H···O contacts (blue dotted lines) in **(1)$_2$[W$_6$O$_{19}$]**. (blue octahedra = WO_6, grey sphere: carbon, pink sphere: phosphor, gold sphere: oxygen, white sphere: hydrogen).

In comparison, the FT-Raman spectra of **(1)$_2$[W$_6$O$_{19}$]** (Figure 2b) and **(1)$_2$[Mo$_6$O$_{19}$]** (Figure S6) exhibit more structured and narrower vibration bands. Typically, the full-width at half maximum of the $\nu_s(CH_3)$ line at 2915 cm^{-1} is 15 and 7 cm^{-1} for **(1)[OTf]** and **(1)$_2$[W$_6$O$_{19}$]**, respectively. In both hybrid POM systems, the symmetric and asymmetric stretching bands of the CH_3 group are shifted to lower frequencies, and the asymmetric stretching vibration is also split in two bands characteristic of a symmetry breaking of the CH_3 group involved in one H-bonding interaction with the POM unit (Figure 1b). Strikingly, the aromatic ν(C-H) band at 3064 cm^{-1} is split with a second maximum band at lower frequency (3058 cm^{-1}) relative to the H-atoms connecting the POM surface. All these results are in direct line with a restriction of the intramolecular motions of the phenyl groups due

Table 1. Photophysical data of **(1)[OTf]** and **$(1)_2[W_6O_{19}]$**.

	λ_{abs} [nm]		λ_{em} [nm]		Φ_F [%]		τ [ns][d]	k_r [$\times 10^7$ s^{-1}][e]	k_{nr} [$\times 10^7$ s^{-1}][f]
	(CH_2Cl_2)	(solid)	(CH_2Cl_2)[a]	(solid)[b]	(CH_2Cl_2)	(solid)[c]			
(1)[OTf]	344, 400	416	546	543	0.5	15	1.42	10.5	59.5
$(1)_2[W_6O_{19}]$	-	416	-	532	-	43	2.42	17.8	23.6

[a]Emission spectra measured at ca. 10^{-5} M CH_2Cl_2 (λ_{ex} = 400 nm). [b]Fluorescence maximum at λ_{ex} = 365 nm. [c]Fluorescence quantum yield in solution has been measured relative to fluoresceine (NaOH, 0.1 M), ϕ_{ref}= 0.9; Fluorescence quantum yield in powder was determined by using a calibrated integrating sphere. [d]Fluorescence lifetime measured at λ_{ex} = 400 nm. [e]Radiative decay rate ($k_r = \Phi_F/\tau$). [f]Nonradiative decay rate ($k_{nr} = 1/\tau - k_r$).

to the strong C–H···O contacts with the highly nucleophilic oxygen POM facets.

The photophysical properties of **(1)[OTf]**, **$(1)_2[W_6O_{19}]$**, and **$(1)_2[Mo_6O_{19}]$** were thoroughly investigated and compared (Table 1). The UV-vis absorption spectrum of **(1)[OTf]** in diluted CH_2Cl_2 solution presents a large band (λ_{abs} = 344 nm) and a shoulder at lower energy (λ_{abs} = 400 nm) assigned to π-π* transitions in the π-extended phosphole (Figure S7).[6] The PL spectrum of **(1)[OTf]** displays a weak emission band centred at 546 nm with a low fluorescence quantum yield (Φ_F) of 0.5%, as expected for AIE-active pentaphenylphosphole derivatives.[14] The diluted solution of **$(1)_2[W_6O_{19}]$** in pure acetonitrile also shows weak luminescence (Figure S8). With gradual increase in the fraction of water e.g., a nonsolvent for **$(1)_2[W_6O_{19}]$**, the emission intensity drastically increases at the same emission wavelength due to aggregate formation. This emission enhancement in the condensed phase likely results from the restricted intramolecular rotation of the phenyl rings of **1^+** involved in multiple noncovalent interactions with the POM units.

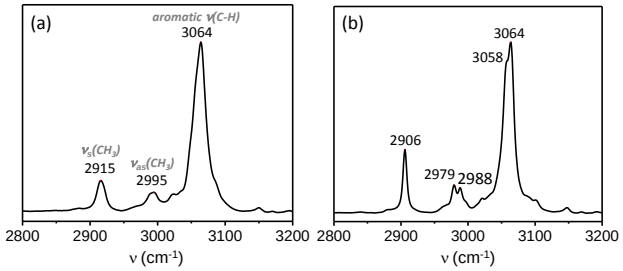

Figure 2. FT-Raman spectra of (a) **(1)[OTf]** and (b) **$(1)_2[W_6O_{19}]$**.

The solid-state UV-vis absorption spectrum of the orange powder of **(1)[OTf]** (Figure 3a) shows an intense absorption band (λ_{max} = 416 nm) associated with the π-π* transition, which tails in the visible. An additional weak band at c.a. 580 nm is also clearly distinguishable and could be assigned to intermolecular effects. This band totally disappeared in diluted solution or when **(1)[OTf]** was embedded in a PMMA matrix (doping rate: 10% in weight, see the Supporting Information for the detailed preparation procedure), in which all intermolecular interactions are disrupted (Figure S9). In stark contrast with **(1)[OTf]**, the solid-state absorption spectra of the yellow powders of **$(1)_2[W_6O_{19}]$** (Figure 3a), and **$(1)_2[Mo_6O_{19}]$** (Figure S10) show that the absorption of **1^+** is much finely structured, and the additional band at 580 nm is not observed. This is in direct line with the POM-induced dilution effect of **1^+** in the hybrid framework that contributes to prevent long-range π-π stacking interactions between the organic luminophores. Importantly, the absorption spectrum of **$(1)_2[W_6O_{19}]$** exhibits a weak overlap, limited to the 275-350 nm range, between the absorption bands of **1^+** and the high-energy O→W ligand-to-metal charge-transfer transitions (LMCT) of the $[W_6O_{19}]^{2-}$ anion (λ_{max} = 280 nm). However, as the $[Mo_6O_{19}]^{2-}$ unit has a LMCT transition lower in energy (λ_{max} = 327 nm) than its tungsten counterpart,[10] the absorptions of both $[Mo_6O_{19}]^{2-}$ and **1^+** moieties in **$(1)_2[Mo_6O_{19}]$** exhibit a significant degree of overlapping in the range 250-450 nm that dramatically impacts its PL performances (see below).

Whereas **(1)[OTf]** is a very weak emitter in diluted solution, its fluorescence is significantly increased in the solid state. **(1)[OTf]** exhibits a broad emission band at 543 nm (Figure 3b) with Φ_F reaching 15%. However, the moderate Φ_F value could be explained owing to the persistence of intermolecular π-π stacking interactions in the crystalline state (Figure S4) that may favor the opposite ACQ effect.

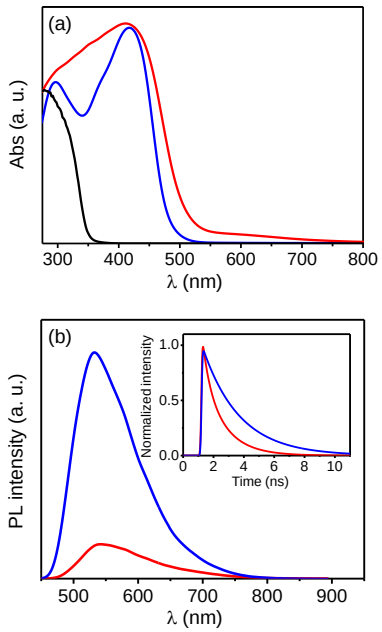

Figure 3. (a) Solid-state UV-vis absorption spectra of **$(1)_2[W_6O_{19}]$** (blue line), **(1)[OTf]** (red line) and $(NBu_4)_2[W_6O_{19}]$ (black line). (b) Solid-state PL spectra of **$(1)_2[W_6O_{19}]$** (blue line) and **(1)[OTf]** (red line) (λ_{ex} = 365 nm). Inset: Corresponding spectrally-integrated emission kinetics (λ_{ex} = 400 nm).

As shown in Figure 3b, **$(1)_2[W_6O_{19}]$** displays a solid-state emission band centred at 532 nm that is slightly blue-shifted of c.a. 10 nm compared to that of **(1)[OTf]**. In the same manner, a blue shift is observed for **(1)[OTf]** embedded in a PMMA matrix (Figure S11). It is worth mentioning that the POM itself does not display any

emission properties. Interestingly, the emission wavelength of **1**$^{+}$ is only moderately modified between the diluted solution, the dilution in a PMMA matrix, and the condensed phase, which is commonly observed for AIE-active heteroles.[2] This singular optical feature contrasts with reported hybrid assemblies combining POMs and other luminescent molecules that often exhibit strong modulations of the emission energy.[10b] This is clearly an advantage in order to design new POM-based emitters with better predictable emission wavelength. Noticeably, the fluorescence quantum yield of **(1)$_2$[W$_6$O$_{19}$]** drastically increases to 43% (~90 times enhanced Φ_F when compared to **1**$^{+}$ in diluted CH_2Cl_2) making **(1)$_2$[W$_6$O$_{19}$]** a strong emitter in the solid state. Clearly, the coupling of the π-extended phospholium with the $[W_6O_{19}]^{2-}$ unit has two beneficial effects. Firstly, the POMs act as efficient spacers that dilute **1**$^{+}$ in the crystal lattice preventing intermolecular π-π interactions and thus diminishing detrimental quenching effects. Secondly, the highly nucleophilic POM surfaces create strong C-H···O contacts with the organic luminophores, drastically exalting the RIR mechanism. To confirm these results, the fluorescence lifetimes of **(1)[OTf]** and **(1)$_2$[W$_6$O$_{19}$]** were thereby measured (inset of Figure 3b). The intensity average decay time (τ_m) is longer for **(1)$_2$[W$_6$O$_{19}$]** (2.42 ns) than for **(1)[OTf]** (1.43 ns). Noticeably, the extracted excited-state radiative decay rate k_r is almost two times higher for **(1)$_2$[W$_6$O$_{19}$]** (17.8×10^7 s^{-1}) than for **(1)[OTf]** (10.5×10^7 s^{-1}), whereas at the same time the nonradiative decay rate k_{nr} drastically decreases from 59.5×10^7 s^{-1} for **(1)[OTf]** to 23.6×10^7 s^{-1} for **(1)$_2$[W$_6$O$_{19}$]**. This quite evidences that intramolecular motions of **1**$^{+}$ are significantly restricted, and that radiative decay is favored in the hybrid POM material. In stark contrast with its tungsten counterpart, **(1)$_2$[Mo$_6$O$_{19}$]** displays a very weak solid-state emission at 532 nm (Figure S10). τ_m dramatically falls to 15 ps, and Φ_F is negligible. Considering that the RIR effects are quite comparable in the $(1)_2[M_6O_{19}]$ (M = Mo, W) series, the fluorescence quenching could be attributed to intermolecular photoinduced electron transfer (PET) between **1**$^{+}$ and the $[Mo_6O_{19}]^{2-}$ unit, due to close proximity of the LUMO levels, as evidenced by the calculation of the Gibbs free energies of the PET (Figure S12 and Table S2). These data nicely illustrate that a careful choice of the POM allows efficiently preparing hybrid emitters using AIE-active cations.

In conclusion, we have synthesized the first supramolecular hybrid materials combining non-conventional POM anions with an AIE-active phospholium. This new assembling strategy allows designing high-performance solid-state emitter such as **(1)$_2$[W$_6$O$_{19}$]** by directing favorably the AIE/ACQ balance through noncovalent interactions. Indeed, the highly nucleophilic POM surfaces strengthen the rigidity of the organic luminophore via strong C-H···O contacts exalting the AIE effect. Besides, the bulky $[W_6O_{19}]^{2-}$ anions strongly prevent the intermolecular π-π stacking interactions responsible of the detrimental ACQ effect. Nevertheless, the isostructural **(1)$_2$[Mo$_6$O$_{19}$]** compound is weakly emissive due to PET from **1**$^{+}$ to the POM, quite underlining that both POM and phospholium energy levels must be well adapted. Furthermore, as the emission wavelength is close to the value measured in diluted solution, this strategy allows preparing hybrid POMs with better predictable emission wavelength. This nicely extends the scope of anion-π^+ engineering to develop solid-state emitters.[5] Finally, as POMs can also exhibit intrinsic photoactive, redox or magnetic properties, this work opens the way towards the design of novel multifunctional hybrid systems.

Acknowledgements

This work was supported by the CNRS, the Université de Nantes, the Université de Rennes 1, the Ministère de l'Enseignement Supérieur et de la Recherche, the LUMOMAT project supported by the *Région des Pays de la Loire*, the French National Research Agency (ANR-16-CE05-0003-01, Heterographene), the China-French associated international laboratory in "Functional Organophosphorus Materials". Y. Molard (ISCR) is thanked for the luminescence quantum yields measurements. T. Roisnel (CDifX, ISCR) is thanked for X-ray diffraction study.

Keywords: Phospholium • Polyoxometalate • Hybrid materials • Aggregation-induced emission • Solid-state luminescence

[1] a) B.-K. An, S.-K. Kwon, S.-D. Jung, S. Y. Park, *J. Am. Chem. Soc.* **2002**, *124*, 14410-14415; b) E. Genin, Z. Gao, J. A. Varela, J. Daniel, T. Bsaibess, I. Gosse, L. Groc, L. Cognet, M. Blanchard-Desce, *Adv. Mater.* **2014**, *26*, 2258-2261; c) J. Gierschner, S. Varghese, S. Y. Park, *Adv. Opt. Mater.* **2016**, *4*, 348-364; d) G. Zhang, J. Lu, M. Sabat, C. L. Fraser, *J. Am. Chem. Soc.* **2010**, *132*, 2160-2162; e) K. Li, B. Liu, *Chem. Soc. Rev.* **2014**, *43*, 6570-6597; f) Y. Tao, K. Yuan, T. Chen, P. Xu, H. Li, R. Chen, C. Zheng, L. Zhang, W. Huang, *Adv. Mater.* **2014**, *26*, 7931-7958; g) H.-C. Su, O. Fadhel, C.-J. Yang, T.-Y. Cho, C. Fave, M. Hissler, C.-C. Wu, R. Reau, *J. Am. Chem. Soc.* **2006**, *128*, 983-995.

[2] a) Aggregation-Induced Emission: Applications; B. Z. Tang, A. Qin, Eds.; Wiley, **2013**; b) Y. Hong, J. W. Y. Lam, B. Z. Tang, *Chem. Soc. Rev.* **2011**, *40*, 5361-5388; c) J. Mei, N. L. C. Leung, R. T. K. Kwok, J. W. Y. Lam, B. Z. Tang, *Chem. Rev.* **2015**, *115*, 11718−11940.

[3] B.-K. An, J. Gierschner, S. Y. Park, *Acc. Chem. Res.* **2012**, *45*, 544-554.

[4] a) F. Würthner, T. E. Kaiser, C. R. Saha-Möller, *Angew. Chem. Int. Ed.* **2011**, *50*, 3376-3410; b) J. Shi, L. E. Aguilar Suarez, S.-J. Yoon, S. Varghese, C. Serpa, S. Y. Park, L. Lüer, D. Roca-Sanjuán, B. Milián-Medina, J. Gierschner, *J. Phys. Chem. C* **2017**, *121*, 23166-23183.

[5] J. Wang, X. Gu, P. Zhang, X. Huang, X. Zheng, M. Chen, H. Feng, R. T. K. Kwok, J. W. Y. Lam, B. Z. Tang, *J. Am. Chem. Soc.* **2017**, *139*, 16974-16979.

[6] a) M. P. Duffy, W. Delaunay, P.-A. Bouit, M. Hissler, *Chem. Soc. Rev.* **2016**, *45*, 5296-5310; b) Y. Ren, T. Baumgartner, *Dalton Trans.* **2012**, *41*, 7792-7800.

[7] a) C. Hay, M. Hissler, C. Fischmeister, J. Rault-Berthelot, L. Toupet, L. Nyulaszi, R. Réau, *Chem. Eur. J.* **2001**, *7*, 4222-4236; b) Y. Ren, T. Baumgartner, *Inorg. Chem.* **2012**, *51*, 2669-2678; c) Z. Wang, B. S. Gelfand, P. Dong, S. Trudel, T. Baumgartner, *J. Mater. Chem. C* **2016**, *4*, 2936-2944; d) P.-A. Bouit, A. Escande, R. Szűcs, D. Szieberth, C. Lescop, L. Nyulászi, M. Hissler, R. Réau, *J. Am. Chem. Soc.* **2012**, *134*, 6524-6527.

[8] a) Y. Ren, W. H. Kan, M. A. Henderson, P. G. Bomben, C. P. Berlinguette, V. Thangadurai, T. Baumgartner, *J. Am. Chem. Soc.* **2011**, *133*, 17014-17026.

[9] a) H. N. Miras, L. Vilà-Nadal, L. Cronin**,** *Chem. Soc. Rev.*, **2014**, *43*, 5679-5699; b) A. Banerjee, B. S. Bassil, G.-V. Röschenthaler, U. Kortz, *Chem. Soc. Rev.*, **2012**, *41*, 7590-7604; c) A. Dolbecq, E. Dumas, C. R. Mayer, P. Mialane, *Chem. Rev*. **2010**, *110*, 6009-6048; d) A. Proust, B. Matt, R. Villaneau, G. Guillemot, P. Gouzerh, G. Izzet, *Chem. Soc. Rev*., **2012**, *41*, 7605–7622.

[10] a) K. Hakouk, O. Oms, A. Dolbecq, J. Marrot, A. Saad, P. Mialane, H. El Bekkachi, S. Jobic, P. Deniard, R. Dessapt, *J. Mater. Chem. C*, **2014**, *2*, 1628-1641; b) P. Bolle, H. Serier-Brault, R. Génois, E. Faulques, A.

Boulmier, O. Oms, M. Lepeltier, J. Marrot, A. Dolbecq, P. Mialane, R. Dessapt, *J. Mater. Chem. C* **2016**, *4*, 11392-11395.
[11] P. G. Rickert, M. R. Antonio, M. A. Firestone, K.-A. Kubatko, T. Szreder, J. F. Wishart, M. L. Dietz, *J. Phys. Chem. B* **2007**, *111*, 4685-4692.
[12] D. Hagrman, P. J. Hagrman, J. Zubieta, *Angew. Chem., Int. Ed*., **1999**, *38*, 3165-3168.
[13] K. Piela, M. Szostak, *J. Phys. Chem. A*, **2012**, *116*, 1730-1745.
[14] a) F. Bu, E. Wang, Q. Peng, R. Hu, A. Qin, Z. Zhao, B. Z. Tang, *Chem. Eur. J.* **2015**, *21*, 4440-4449; b) A. Fukazawa, Y. Ichihashi, S. Yamaguchi, *New J. Chem.* **2010**, *34*, 1537-1540.

Entry for the Table of Contents (Please choose one layout)

COMMUNICATION

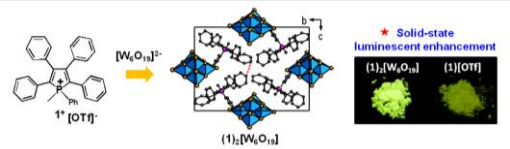

The first assemblies of an aggregation-induced emission (AIE)-active cationic phospholium with the $[M_6O_{19}]^{2-}$ (M = Mo, W) polyoxometalate anions through noncovalent interactions was designed. This innovative coupling allows drastically exalting the solid-state luminescence of the organic luminogen by directing favorably the AIE/ACQ balance.

Patricia Bolle, Yohan Chéret, Claire Roiland, Lionel Sanguinet, Eric Faulques, Hélène Serier-Brault, Pierre-Antoine Bouit, Muriel Hissler,* and Rémi Dessapt**

Page No. – Page No.

Strong solid-state luminescence enhancement in supramolecular assemblies of polyoxometalate and "Aggregation-Induced Emission"-active phospholium